<Оптика атмосферы и океана>, **6**, N 3 (1993)

УДК 535.33

P. Blau

ANALYSIS OF THE IMPEDANCE OF A COAXIAL, LARGE–BORE COPPER VAPOR LASER

The impedance of the laser head of a 100 W copper–vapor laser is investigated. The laser head is of a coaxial geometry which is commonly used for longitudinally electrically excited, pulsed–gas lasers.

The plasma conductivity is estimated using the available data on plasma parameters. The effect of radial gradient of the gas–temperature is considered. The tube inductance and capacitance are estimated and the combined effect is demonstrated. The skin–effect is considered. A method to calculate the exact influence of the skin–effect on the tube impedance is presented.

The full calculation procedure is demonstrated for the case of a 100 W, 8 cm diameter, copper vapor laser. The consequent impedance is used to calculate the laser current under given excitation conditions. Very good agreement exists between the calculated and measured laser current.

An optimal metal–sleeve diameter with respect to power matching is found.

1. introduction

The copper vapor laser (CVL) is a pulsed–electric–discharge pumped laser. Development of an excitation circuit that will efficiently transfer the electrical power into the plasma of CVL is one of the difficult tasks in high power CVL improvement. The reason for this is that to get efficient excitation, high power should be supplied during short intervals, of the order of 100 ns [1]. Typical values for the efficiency of the excitation circuit are 50%, i.e., only half of the power delivered from the power supply is finally deposited in the plasma. The residual power is absorbed by the circuit components, and results in their fast deterioration. Knowledge of the impedance of the laser and the parameters that affect is essential for optimization of the power matching.

Most of the published works on this issue, model the laser impedance as a resistance in series with a constant inductance[2], or neglect the inductance altogether [3]. In some of those works the parameters were estimated in a very simplified manner, in others they were deduced from the measured current waveform, but the actual empirical parameters can be provided only for a specific working system and are relevant only to the specified working conditions. Moreover, a recent work [4] has shown that constant parameters cannot satisfactorily explain the behavior of our laser.

Another approach to laser impedance is the physical approach. In this approach simulation of the plasma kinetics is utilized in order to calculate the time–varying plasma conductivity [5–7]. This approach offers better insight into the physical properties of the laser. The main drawback of this method, from our point of view, is the time–consuming calculation required in order to solve a large number of kinetic equations. In some of the previous works radial uniformity and therefore constant inductance was assumed. This assumption is clearly not correct for a large–bore CVL [5] and in fact doubtful even for a small–bore one [8].

Effects regarding the laser tube capacitance are considered here for the first time. We present a method to calculate the laser tube inductance and capacitance and the combined effect using transmission line formulation. The plasma conductivity is assumed to be constant in time. The time dependence of the impedance caused by radial field penetration (skin–effect) is considered.

The theoretical results are compared to measurements performed on a 100 W, 170 cm long, 8 cm diameter CVL. The structure of the laser head is described in Fig. 1. The laser head is of coaxial geometry. An alumina lasing tube is surrounded by an alumina thermal insulator. This tube is enclosed in a quartz tube and electrically shielded by a metal sleeve. A detailed description of the laser, its excitation circuit, and working parameters is given elsewhere [1].

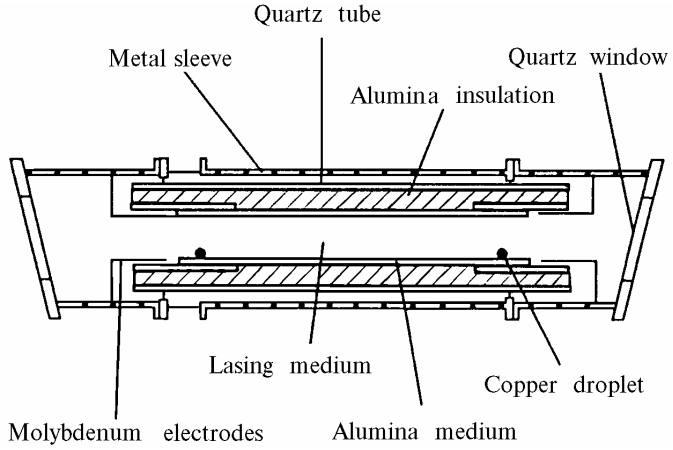

Fig. 1. The structure of the laser head

II. **Theoretical considerations**

A. The resistance of the laser head. The resistive element is the plasma itself. The plasma resistance is a result of collisions of the conducting electrons with plasma constituents. Estimation of the plasma conductivity is obtained in the following way [9]: The plasma conductivity is given by

$$\sigma = \frac{n_e e^2}{m_e \nu_m}, \tag{1}$$

where n_e is the electron number density, e and m_e are the electron charge and mass, and ν_m is the collision frequency for momentum transfer, ν_m is given by

$$\nu_m = N \langle v \rangle \sigma_m, \tag{2}$$

where N is the number density of atoms, $\langle v \rangle$ is the average electron velocity and σ_m is the cross section for momentum transfer. The gas density is deduced from its pressure and temperature. The electron velocity is deduced from its energy. If there are more than one type of atoms in the gas the frequencies of collisions with different atoms are summed.

The main constituents in our plasma are neon, hydrogen, and copper atoms. Typical number densities, momentum transfer cross sections, and the resulting collision frequencies with these atoms are listed in Table I. The atom density corresponds to gas temperature of 1880 K as the temperature near the tube wall. Electron energy of 1 eV is assumed.

Table 1

Collision frequency with plasma ingredients.

Atom	Number density, cm^{-3}	Momentum transfer cross section, cm^2	Collision frequency, sec^{-1}
Neon	$4 \cdot 10^{17}$	$1{,}5 \cdot 10^{-16}$ [a]	$3{,}6 \cdot 10^{9}$
Hydrogen	$4 \cdot 10^{15}$	$3 \cdot 10^{-15}$ [b]	$7{,}2 \cdot 10^{8}$
Copper	$8 \cdot 10^{14}$	$6 \cdot 10^{-16}$ [c]	$2{,}9 \cdot 10^{7}$

[a] From Ref. 10; [b] From Ref. 16; [c] From Ref. 17

As can be seen from Table 1 the dominant processes are collisions with neon atoms. The electron energy in our plasma varies between 0.3 eV, before the excitation pulse, and 5 eV at the pulse maximum [5]. The momentum transfer cross section for neon can be considered constant in this range and equals $1{,}5 \cdot 10^{-16}\,cm^2$ [10]. Therefore, only the dependence of conductivity on the neon and electron number densities, and on the average electron velocity is considered. Under constant gas pressure, the gas number density is inversely proportional to the gas temperature and is given by

$$N = 3{,}536 \cdot 10^{16} \frac{273}{T} P\left[\frac{\mathrm{cm}^{-3}}{\mathrm{Torr}}\right], \tag{3}$$

where P is the gas pressure in Torr and T is the gas temperature in K. High radial temperature gradients exist in the CVL plasma. The gas temperature near the axis is more than twice the gas temperature near the wall [5]. Thus, the conductivity is not uniform. Another factor, that influences the final resistance, is the skin–effect which restricts the current to part of the tube. In the final calculation we take into account these phenomena.

B. The inductance of the laser head. Estimate of the tube inductance can be obtained assuming the electric current density in the plasma to be uniform. The inductance is then given by [11]

$$L_{\mathrm{uniform}} = \frac{\mu_0 l}{2\pi}\left\{\frac{1}{4} + \ln\frac{b}{a}\right\}, \tag{4}$$

where μ_0 is the permeability of free space, l is the tube length, a is the inner diameter of the lasing tube, and b is the inner diameter of the metal sleeve. From Eq. (4) one can see that the inductance decreases as the ratio b/a decreases. For this reason, the tendency was to minimize the outer sleeve diameter for a given tube diameter in order to minimize the laser inductive impedance, thereby increasing the current in the laser for a given applied voltage and improving power matching. This concept is not always correct as will be demonstrated later.

The radial dependence of the conductivity and the skin–effect result in nonuniform current density. In this case Eq. (4) is not valid. If the current density profile has a ring shape, the inductance decreases and is given by [4]

$$L_{\mathrm{ring}} = \frac{\mu_0 l}{2\pi}\left\{\ln\frac{b}{a} + \frac{c^4}{(a^2 - c^2)^2}\ln\frac{a}{c} + \frac{a^2 - 3c^2}{4(a^2 - c^2)}\right\}, \tag{5}$$

where c is the inner diameter of the ring. The minimum value of the inductance is obtained, if the current flows in a thin layer near the wall ($c \to a$). The inductance is then given by

$$L_{\mathrm{min}} = \frac{\mu_0 l}{2\pi}\ln\frac{b}{a}. \tag{6}$$

This is the case for a current that oscillates at a very high frequency. The current chooses a path with low inductance, because the inductive impedance rises with frequency. This is essentially the skin–effect. The inductance can also exceed over the value given by Eq. (4) if the current density near the tube axis is higher than the current density near the wall. This can occur as a result of increased conductivity caused by increased gas temperature near the axis. In the general case the inductance should be calculated using the time–dependent current density profile.

C. Skin–effect. The skin–effect is obtained from the following Maxwell equations:

Faraday's law

$$\nabla \times E = -\frac{\partial B}{\partial t}. \tag{7}$$

Ampere's law

$$\nabla \times B = \mu_0 J + \mu_0 \frac{\partial}{\partial t}(\varepsilon_0 E). \tag{8}$$

In our system $\frac{\partial}{\partial t}(\varepsilon_0 E) \ll J$, therefore, the displacement current is neglected. By taking the curl of the first equation and substituting it into the second equation, we obtain

$$\nabla\times(\nabla\times E) = -\frac{\partial}{\partial t}(\nabla\times B) = -\mu_0\frac{\partial J}{\partial t}, \tag{9}$$

or

$$\nabla(\nabla\cdot E) - \nabla^2 E = -\mu_0\frac{\partial J}{\partial t}. \tag{10}$$

Assuming the plasma quasi neutrality ($\nabla\cdot E = \frac{\rho}{\varepsilon_0} = 0$), we finally have

$$\nabla^2 E = \mu_0\frac{\partial J}{\partial t} = \mu_0\frac{\partial(\sigma E)}{\partial t}, \tag{11}$$

where σ is the plasma conductivity.

This is a diffusion equation. In cylindrical coordinates, assuming axial and longitudinal symmetry, Eq. (11) reads

$$\frac{\partial^2 E}{\partial r^2} + \frac{1}{r}\frac{\partial E}{\partial r} = \mu_0\frac{\partial(\sigma E)}{\partial t}. \tag{12}$$

If we assume constant conductivity and solution of the form $E = E(r)e^{i\omega t}$, the equation for $E(r)$ is

$$\frac{\partial^2 E(r)}{\partial r^2} + \frac{1}{r}\frac{\partial E(r)}{\partial r} = i\,\omega\,\mu_0\,\sigma\,E(r). \tag{13}$$

Analytical solution exists under the assumption of uniform conductivity. In this case Eq. (13) can be written as follows:

$$\frac{\partial^2 E(x)}{\partial x^2} + \frac{1}{x}\frac{\partial E(x)}{\partial x} = iE(x), \tag{14}$$

where $x = r/\delta$ and $\delta = (\omega\sigma\mu_0)^{-1/2}$.

Equation (14) is one of the forms of the Bessel equation and its solution is given by [12]

$$E(x) = E_0 J_0\left(x\,e^{\frac{3\pi i}{4}}\right), \tag{15}$$

where E_0 is a complex constant and J_0 is the Bessel function of the zeroth order. The other solution is not physical, because it diverges as $x \to 0$. The real and imaginary parts of $J_0\left(x\,e^{\frac{3\pi i}{4}}\right)$ are denoted by Ber(x) and Bei(x), where [12]

$$\mathrm{Ber}(x) = 1 - \frac{(x/2)^4}{2!^2} + \frac{(x/2)^8}{4!^2} - \ldots = \frac{1}{\pi}\int_0^{\pi}\cos\left[\frac{x}{\sqrt{2}}\sin\theta\right]\cosh\left[\frac{x}{\sqrt{2}}\sin\theta\right]d\theta, \tag{16}$$

$$\mathrm{Bei}(x) = (x/2)^2 - \frac{(x/2)^6}{3!^2} + \frac{(x/2)^{10}}{5!^2} - \ldots = \frac{1}{\pi}\int_0^{\pi}\sin\left[\frac{x}{\sqrt{2}}\sin\theta\right]\sinh\left[\frac{x}{\sqrt{2}}\sin\theta\right]d\theta. \tag{17}$$

The complex solution means, that both the magnitude and phase of the field are changing with the distance from the axis. To demonstrate this, the solution in polar representation is presented in Fig. 2.

$$R(x) = \sqrt{\mathrm{Ber}(x)^2 + \mathrm{Bei}(x)^2}\,,\ \Theta(x) = \tan^{-1}\left(\frac{\mathrm{Bei}(x)}{\mathrm{Ber}(x)}\right). \tag{18}$$

In our system $\delta \approx R/2$, where R is the tube radius, hence x is approximately 2 near the tube wall. Thus, intensity of the field at the axis is about 20% less than of the field near the wall and the phase of the field near the wall precedes by about 1 rad the field phase at the axis. In our system the typical frequency is $2 \cdot 10^7$ rad/sec, thus, a delay of about 40 ns exists between the field near the wall and the field at the axis. This is a well–known phenomenon in large–bore CVL's and is observed also in the laser radiation.

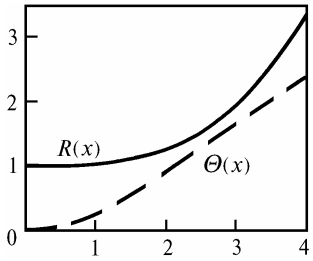

Fig. 2. Field amplitude (solid line) and phase (dashed line) relative to amplitude and phase on axis. X is the distance from axis in units of $\delta = (\omega\sigma\mu_0)^{-1/2}$

The field is given by

$$E\,(r, t) = E_0\, J_0\left(r/\sigma\, \mathrm{e}^{\frac{3\pi i}{4}}\right) \mathrm{e}^{i\omega t}\,. \tag{19}$$

The current density is then

$$J\,(r, t) = E_0 \cdot \sigma \cdot J_0\left(r/\sigma\, \mathrm{e}^{\frac{3\pi i}{4}}\right) \mathrm{e}^{i\omega t}\,. \tag{20}$$

The total current is obtained by integration

$$I_{\mathrm{total}}(t) = \int_0^R 2\pi J(r, t)\, r\mathrm{d}r = \frac{2\pi}{\left(\mathrm{e}^{\frac{3\pi i}{4}}/\delta\right)^2}\sigma E_0 \int_0^Y J_0(y) y\, \mathrm{d}y\, \mathrm{e}^{i\omega t}, \tag{21}$$

where $Y = \dfrac{R}{\delta}\,\mathrm{e}^{\frac{3\pi i}{4}}$. But for the Bessel function [12]

$$\int x\, J_0(x)\mathrm{d}x = x\, J_1(x)\,, \tag{22}$$

where $J_1(x)$ is the Bessel function of the first order. Thus, finally we have

$$I_{\mathrm{total}}(t) = \frac{2\pi R\delta}{\mathrm{e}^{\frac{3\pi i}{4}}}\,\sigma\, E_0\, J_1\left(\frac{R}{\delta}\,\mathrm{e}^{\frac{3\pi i}{4}}\right) \mathrm{e}^{i\omega t}\,. \tag{23}$$

The impedance is defined as the relation between the applied voltage and the total current. To calculate it, we use the integral form of the Maxwell equations.

$$\oint_c E\,\mathrm{d}\,l = -\frac{\partial}{\partial t}\int_s B\,\mathrm{d}\,s\,, \tag{24}$$

$$\oint_c B \,\mathrm{d}\, l = \int_s \mu_0 J \,\mathrm{d}\, s \,, \tag{25}$$

where $\oint_c$ denotes integration over a closed path c, and $\oint_S$ denotes integration over the surface confined within this line. The integration of Eq. (25) is performed over a circle of radius r around the laser axis, if r is larger than the tube radius and smaller than the metal–sleeve radius, the surface integral on the right–hand side of Eq. (25) yields the total laser current. Assuming axial symmetry for the magnetic field, we obtain

$$2\pi r B(r) = \mu_0 I_{\text{total}} \,. \tag{26}$$

The integration of Eq. (24) is performed over the path of minimum inductance, this is the path along the laser near the tube wall and back along the metal sleeve. The magnetic field penetrating through the closed surface is taken from Eq. (26), the end effect is neglected. The electric field in the metal sleeve is assumed to be zero, but we have to take into account the voltage applied to the laser tube. Thus, we obtain

$$E_{\text{wall}}\, l - V = -\frac{\partial}{\partial t} \int_{R_T}^{R_s} \frac{\mu_0 I_{\text{total}}}{2\pi r} \,\mathrm{d}\, r l = \frac{\mu_0 l}{2\pi} \ln\left(\frac{R_s}{R_T}\right) \frac{\partial I_{\text{total}}}{\partial t} \,, \tag{27}$$

where V is the applied voltage, E_{wall} is the electric field near the tube wall, R_T and R_s are the tube and sleeve radii. The current density near the wall is $J_{\text{wall}} = \sigma \cdot E_{\text{wall}}$. The coefficient on the right–hand side of Eq. (27) is what was regarded above (Eq. 6) as L_{min}, the minimum tube inductance. Therefore, we can write

$$V = \frac{J_{\text{wall}}\, l}{\sigma} + L_{\text{min}} \frac{\partial I_{\text{total}}}{\partial t} \tag{28}$$

or for harmonic current

$$V = \frac{J_{\text{wall}} \cdot l}{\sigma} + i\,\omega\, L_{\text{min}}\, I_{\text{total}} \,. \tag{29}$$

The impedance is then given by

$$Z = \frac{V}{I_{\text{total}}} = \frac{J_{\text{wall}}}{I_{\text{total}}} \frac{l}{\sigma} + i\,\omega\, L_{\text{min}} \,. \tag{30}$$

Using the explicit expression for the total current and the field near the wall from above we have

$$Z = \frac{J_0\left(\frac{R_T}{\delta} \mathrm{e}^{\frac{3\pi i}{4}}\right) \mathrm{e}^{\frac{3\pi i}{4}}}{2\pi R_T \delta J_1\left(\frac{R_T}{\delta} \mathrm{e}^{\frac{3\pi i}{4}}\right)} \frac{1}{\sigma} + i\,\omega\, \frac{l\,\mu_0}{2\pi} \ln\left(\frac{R_s}{R_T}\right). \tag{31}$$

The real part of the impedance is the total resistance and the imaginary part is the inductive impedance, i.e., $\omega \cdot L$. Figure 3 shows the resistance and inductance as functions of frequency using typical parameters of our system. The resistance increases with frequency, because the skin depth decreases and the current is restricted to smaller section of the tube. The inductance in the limit of high frequency converges to L_{min} as was expected. For low frequency the inductance converges to the value of L_{uniform} as is calculated assuming current density (Eq. 4), because the skin depth is larger than the tube radius.

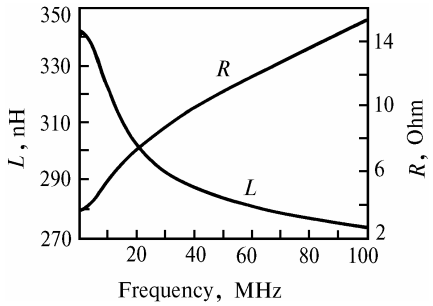

Fig. 3. Resistance and inductance versus frequency calculated from Eq. (31), i.e., assuming uniform conductivity, with typical parameters for our laser

The above calculation is correct, if the conductivity is uniform. More realistic calculations require the use of the radial dependent conductivity. In this case, different equation for the radial dependence of the electric field is

$$\frac{d^2 E(r)}{d r^2} + \frac{1}{r}\frac{d E(r)}{dr} = i\,\omega\,\mu_0 \sigma(r)\,E(r)\,, \tag{32}$$

where $\sigma(r)$ is the radial dependent conductivity. The general solution (omitting a constant factor that drops later) is given by the following integral:

$$E(r) = i\omega\,\mu_0 \int_0^r \frac{1}{r_1}\left[\int_0^{r_1} r_2\,\sigma(r)\,E(r) d\,r_2\right] d\,r_1\,. \tag{33}$$

This can be verified by doubly differentiating Eq. (33). The equation is solved numerically using the radial dependent conductivity in order to find $E(r)$. The total current I_{total} is calculated by integration

$$\frac{I_{\text{total}}}{e^{i\omega t}} = \int_0^{R_T} E\,(r)\,\sigma\,(r)\,2\pi r\,\mathrm{d}\,r\,. \tag{34}$$

The current density near the wall is $J_{\text{wall}} = E\,(R_T)\,\sigma(R_T)\,e^{i\omega t}$ and the impedance is given by

$$Z = i\,\omega\,L_{\min} + \frac{I_{\text{wall}}}{I_{\text{total}}}\frac{1}{\sigma(R_T)} = i\,\omega\,L_{\min} + \frac{E(R_T)\,l}{\int_0^{R_T} E(r)\,\sigma(r)\,2\pi r d\,r}\,. \tag{35}$$

To demonstrate the effect of nonuniform conductivity, Table 2 shows the values of total resistance and inductance calculated for our system in three ways. The first and last lines are calculated assuming uniform conductivity but with different values of the conductivity. At higher conductivity the resistance is, of course, lower. The inductance is lower because of the decrease in skin depth. The central line is calculated assuming radial (gas temperature) dependent conductivity. The resistance in this case is lower than in the other two due to the increase in conductivity. The inductance is higher than in the other two cases due to the increase in current density in the high temperature and high conductivity region near the tube axis, the region with higher inductance.

The first and third lines in the table are calculated assuming that the plasma conductivity is uniform and equals the conductivity near the wall using Eq. (31) with typical parameters from our laser. The second line is calculated using Eq. (35) and assuming that the conductivity depends on the gas temperature and is therefore not uniform but radial dependent.

Table 2

Calculated laser resistance and inductance

Method	Conductivity near wall ($\Omega^{-1} \cdot cm^{-1}$)	Resistance, (Ω)	Inductance, (nH)
Uniform conductivity	1	3,83	339
Temperature dependent conductivity	1	2,53	352
Uniform conductivity	1,5	2,74	335

D. The capacitance of the laser head. Radial electric field exists in the laser head only on the quartz tube and the spacing between this tube and metal sleeve. The alumina components are not isolated from the plasma and are conducting at the working temperature (for description of the laser head structure refer to Sec. 1). This implies that capacitance exists only on the first two components. The capacitance of two coaxial tubes is given by [11]

$$C_{\text{tube}} = \frac{2\pi\varepsilon\, l}{\ln\,(r2/r1)}, \tag{36}$$

where ε is the dielectric constant of the medium between them, l is the tubes length, $r2$ and $r1$ are the radii of the outer and inner tube. The capacitance increases as the ratio $r2/r1$ decreases and the dielectric constant of the insulating medium increases. The capacitances on the quartz tube and on the spacing between it and the sleeve should be regarded as connected in series.

E. The total impedance. To evaluate the combined effect of the resistance, inductance, and capacitance, the problem of the impedance of a short transmission line with losses should be solved, assuming a transmission line with the following parameters per unit length: resistance R, inductance L, and capacitance C. The equivalent circuit is shown in Fig. 4.

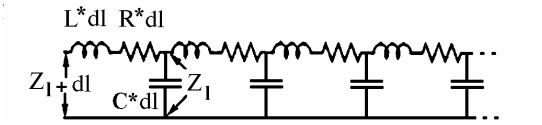

Fig. 4. Equivalent circuit for a transmission line with losses. The impedance of a line $l + dl$ units long can be expressed as a function of the impedance of a line l units long and the resistance, inductance, and capacitance per unit length.

If the impedance of a line of length l is Z_l, the impedance of a line of length $l + dl$ is

$$Z_{l+dl} = R\,dl + i\omega\, L\,dl + \left(i\omega\, C\,dl + \frac{1}{Z_l}\right)^{-1}. \tag{37}$$

The derivative of Z with respect to l is defined as

$$\frac{dZ}{d\,l} = \lim_{dl\to 0}\left[\frac{Z_{l+dl} - Z_l}{dl}\right] = \lim_{dl\to 0}\left[\frac{Rdl + i\omega\, L\,dl + Z_l\dfrac{1 - i\omega\, C\,dl\,Z_l}{1 + (\omega\, C\,dl\,Z_l)^2} - Z_l}{dl}\right]. \tag{38}$$

As a result we obtain the following differential equation for the impedance:

$$\frac{dZ}{d\,l} = R + i\,\omega\, L - i\,\omega\, C{\cdot}Z^2. \tag{39}$$

The general solution of this equation, with a boundary condition $Z(l_0) = \eta$, is [13]

$$Z(l) = \frac{\eta\sqrt{-i\omega C\,(R + i\omega L)} + (R + i\omega L)\tan(\sqrt{-i\omega C\,(R + i\omega L)}{\cdot}(l - l_0))}{\sqrt{-i\omega C\,(R + i\omega L)} + i\omega C{\cdot}\eta\tan(\sqrt{-i\omega C\,(R + i\omega L)}{\cdot}(l - l_0))}. \tag{40}$$

For infinitely long line the solution is

$$Z = \sqrt{\frac{R + i\,\omega\,L}{i\,\omega\,C}}, \tag{41}$$

which is the classical value of transmission line impedance. For the boundary condition $Z(0) = 0$, which is our case, the solution is

$$Z(l) = \sqrt{-\frac{R + i\,\omega\,L}{i\,\omega\,C}}\,\tan\left(l\sqrt{-i\,\omega\,C\,(R + i\,\omega\,L)}\right). \tag{42}$$

To demonstrate the effect of the transmission line (or parasitic capacitance), Fig. 5 shows the real and imaginary parts of the impedance obtained for the parameters of our laser with and without consideration of the capacitance. When the capacitance is considered, resonance phenomenon occurs. At the resonance frequency the imaginary impedance vanishes. Below this frequency both parts of the impedance increase. Beyond this frequency the imaginary part changes sign what means the change from inductive to capacitive behavior.

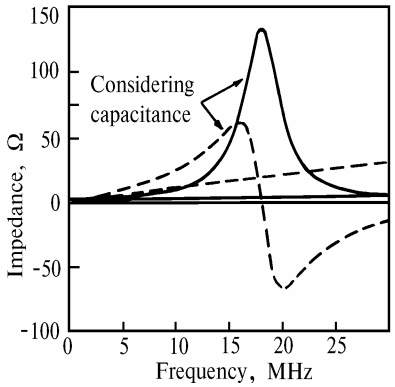

Fig. 5. The real (solid line) and imaginary (dashed line) parts of the calculated laser impedance with and without considering the capacitance and transmission–line effect

III. Application to copper vapor lasers

A. System parameters and theoretical results. The neon pressure in our laser is 76 Torr. The gas temperature is 1800°K near the tube walls and about 4300°K along its axis [14].

The time averaged electron number density measured at the laser axis is $1{,}3 \cdot 10^{13}$ cm^{-3} [14]. A maximum electron density of $4 \cdot 10^{13}$ cm^{-3} at about 1 μsec after the excitation pulse was obtained in a model of a similar laser [5]. The electron energy obtained in this model is 0.3 eV before the excitation pulse and 5 eV at its maximum. Table III demonstrates some conductivity values obtained using these parameters. As can be seen the conductivity value can differ by about an order of magnitude for different time and points in the tube.

Table 3

Estimated plasma conductivity from various estimations of plasma parameters. The parameters correspond to different time and points in the plasma.

Location	Time	Gas temperature, K	Electron density, (10^{13} cm^{-3})	Electron energy, (eV)	Conductivity, (Ω^{-1}·cm^{-1})
Near wall	Before pulse	1800[a]	1.5[a]	0.3[b]	2.1
Near wall	During the pulse	1800[a]	1.5[a]	5[b]	0.52
On axis	During the pulse	4300[a]	1.5[a]	5[b]	1.2
On axis	After pulse	4300[a]	4[b]	1[b]	7.4

[a] From Ref. 14; [b] From Ref. 5;

We take into account the radial dependence of the conductivity resulting from the gas temperature profile. For this purpose the gas temperature is calculated with the assumption of uniform power deposition and given by [5]

$$T(r) = \left[T_{\omega}^{m+1} + \frac{P\,(m+1)}{4\lambda_0} (R^2 - r^2) \right]^{\frac{1}{1+m}}, \tag{43}$$

where T_ω is the wall temperature (1800°K in our laser), P is the power deposited per unit volume (about 1,5 W $\cdot$ cm^{-3}), R is the tube radius (4 cm), and λ_0 and m are constants related to the thermal conductivity of the gas. The thermal conductivity is given by [15]

$$\lambda = \lambda_0 T_g^m, \tag{44}$$

where T_g is the gas temperature. For neon $\lambda_0 = 9{,}6 \cdot 10^{-6} \left[\frac{W}{K \cdot \mathrm{cm}} \right]$ and $m = 0{,}685$. The radial dependence of the electric conductivity resulting from radial gradients of the electron number density and velocity was not accounted because of lack of data.

The best agreement between the calculated and measured laser current was reached when assuming plasma conductivity of 60 $(\Omega \cdot \mathrm{m})^{-1}$ near the tube wall. This value of conductivity corresponds to gas temperature of 1800°K, the actual wall temperature, to electron density of $1.3 \cdot 10^{13}$ cm^{-3}, the actual measured average electron density, and to the electron energy of 3 eV, 60% of the maximum value obtained in Ref. 5.

The estimated parameters for our tube are:

Minimum inductance, using Eq. (6): $L_{\min}$ = 238 nH.
Inductance assuming uniform current, using Eq. (4): L_{uniform} = 323 nH.
Total capacitance, using Eq. (36) and adding the quartz tube capacitance and the capacitance of the spacing between quartz and sleeve tubes in series: 0,63 nF.

Figure 5 shows the real and imaginary parts of the impedance as obtained using the full calculation procedure.

B. Experimental procedure. In order to examine the theoretical results, measurement of the impedance which is isolated from influence of other circuit component is required. A method that meets this demand and also the bandwidth demands of the measurement was described by Druckmann [4]. The method utilizes measurement of the current partition between the laser head and the capacitor that is connected in parallel to it in a standard circuit (peaking capacitor) [1], see Fig. 6. The currents are measured with the W series current–viewing–resistors from T&M Research Products. Those resistors are 0.2% accurate and have a bandwidth of 400 MHz. The signals are sampled with a TEK 11201, 400 MHz digitizing oscilloscope and transmitted to a computer for processing.

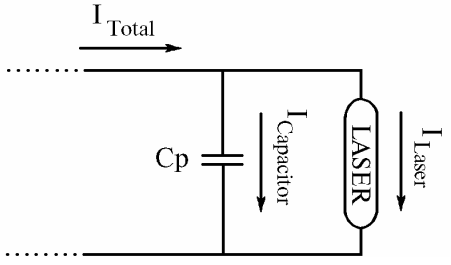

Fig. 6. The impedance measurement circuit. The total current that arrives from the excitation circuit is measured and also the part of it that flows through the laser. The time (frequency) dependent current partitioning factor is a function of the laser impedance

The parallel capacitor is 4 nF, UHV–11A ceramic capacitor from TDK. Its capacity has low voltage and frequency dependence but high temperature dependence. The temperature of the capacitor was measured and the capacitance was evaluated according to the capacitor data–sheet.

Figure 7 shows typical total excitation current and the laser current signals. The voltage is calculated from the charge on the peaking capacitor which is obtained by integrating the net current through it.

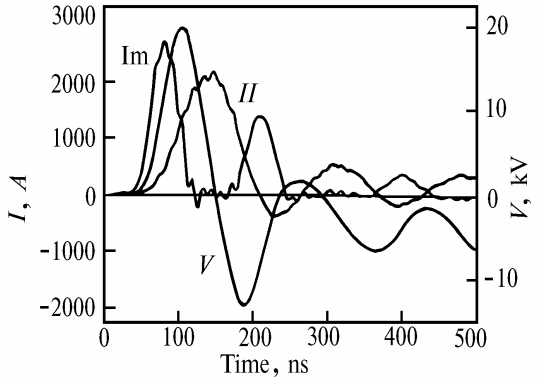

Fig. 7. Typical total (Im) and laser (Il) measured currents. The voltage (V) is calculated by integrating the net current through the capacitor

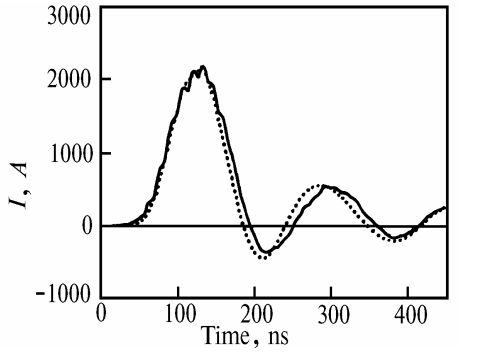

Fig. 8. Measured (solid line) and calculated ((dotted line) laser current

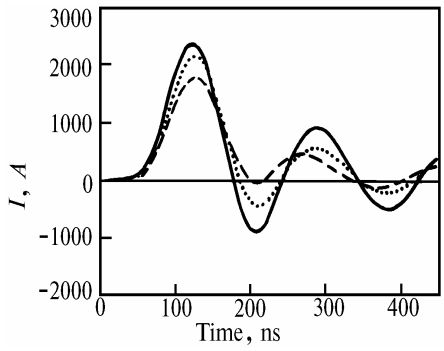

Fig. 9. Laser current calculated with different conductivity near the wall. Solid line – 120 $(\Omega m)^{-1}$, dotted line – 60 $(\Omega m)^{-1}$, and dashed line – 30 $(\Omega m)^{-1}$

Figure 8 demonstrates the agreement between measured and calculated laser current. The theoretical result is obtained as follows. The full, frequency dependent laser impedance is calculated as above. The partitioning factor between the laser and the total excitation current is

$$\frac{I_l}{I_{ex}} = \frac{Z_l \,||\, Z_c}{Z_l} = \frac{Z_c}{Z_l + Z_c}, \tag{45}$$

where Z_l is the laser impedance and Z_c is the impedance of the peaking capacitor. The frequency spectrum of the measured total current is obtained using fast Fourier transform and is multiplied by the partitioning factor to get the frequency spectrum of the laser current. Inverse fast Fourier transform is used to obtain the laser current.

The sensitivity of the results to the value of the conductivity near the wall is demonstrated in Fig. 9. The same effect of the laser current will be observed if the gas pressure is varied.

IV. Discussion and conclusion

Good agreement exists between the measured and calculated current waveforms. The peak current value is sensitive to the exact value of the conductivity which is assumed. Time dependence of the conductivity was not considered. A good agreement with measurements proves that in our case the time dependence of the laser impedance is dominated by the field penetration process. This is connected with the significance of the inductance in the total impedance. The conductivity value of 60 $(\Omega \cdot m)^{-1}$, which gives the optimal agreement with

measurements, implies that the electron energy changes rapidly with the applied field. The electron number density, on the other hand, changes more slowly. The main disagreement between measurements and calculations is in the width of the first peak. The width of the measured current is somewhat wider than the predicted one. This implies that the true inductance is somewhat higher than the predicted one. This can be explained as follows: we have assumed uniform electron number density. In fact, during the time interval between excitation pulses the recombination between electrons and ions occurs. This process is faster near the wall than on the axis, therefore at the beginning of the pulse the electron density near the wall (and thus the conductivity) is much lower. To demonstrate the effect of this on the resulting current, Fig. 10 shows the result of a calculation that assumes current to be flowing in a region of only 7 cm in diameter. The agreement with the measured current is much better in this case.

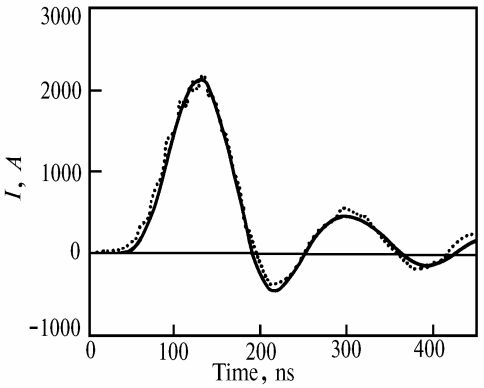

Fig. 10. Measured laser current (dotted line) and laser current calculated assuming that the current flows only in a region of 7 cm in diameter

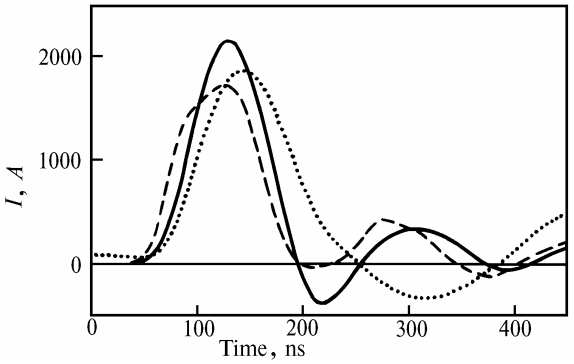

Fig. 11. Calculated laser current with different metal sleeve diameters. Dotted line – 40 cm, solid line – 20 cm, and dashed line – 14.5 cm diameter

Another important effect that can be obtained with the above calculation is the effect of modifications in the sleeve diameter. Figure 11 shows the current obtained for different sleeve diameters. For a narrower sleeve the current peak increases because of the decrease in the inductance, but there is an optimal sleeve diameter below which the current pulse is smeared and its peak decreases. This is a result of the increase in capacitance and it occurs also when increasing the dielectric constant of the medium between the quartz tube and the metal sleeve. This phenomenon was also observed experimentally.

1. Gabay S., Blau P., Lando M., Druckman I., Horvitz Z., Yfrah I., Hen I., Miron E., Smilanski I. // Optical and Quantum Electron. 1991. V. 23, P. 485.
2. Astadjov D.M., Vuchkov N.K., Sabotinov N.V. // IEEE J. Quantum Electron. 1988. T. 24. C. 1927.
3. Batenin V.M., Burmakin V.A., Vokhmin P.A., Evtyunin A.I., Klimovskii I.I., Lesnoi M.A., Selezneva L.A. // Sov. J. Quantum Electron. 1977. V. 7. P. 891.
4. Druckmann I. // IEEE J. Quantum Electron, submitted..
5. Kushner M.J. and Warner B.E. // J. Appl. Phys. 1983. V. 54, P. 2970.
6. Artem'ev A.Yu. et al. // Sov. J. Quantum Electron. 1983. V. 13. P. 936.
7. Aoki N., Kimura H., Konagai C, Shirayama S., Miyazawa T., Takahashi T. // Proc. SPIE. 1991. V. 1412. P. 2.
8. Zapesochnyi I.P., Kel'man V.A., Klimovskii I.I., Selezneva L.A., Fuchko V.Yu. // High Temp. 1989. V. 26. P. 505.
9. Cherrington B.E. Caseous Electronics and Gas Lasers (Pergamon; Oxford, 1979).
10. Bederson B., Kieffer L.J. // Rev. Mod. Phys. 1971. V. 43. P. 601—640.
11. Corson D.R., Lorrain P. Introduction to Electromagnetic Fields and Waves. W. H. Freeman and Company, San Francisco and London, 1982.
12. Spiegel M.R. Mathematical Handbook, Schaum's Outline series. McGraw-Hill Book Company. New York, 1968.
13. Kamke E. Differentialgleichungen. Akademishe Verlag, Leipzig, 1951.
14. Blau P., Smilanski I., Rosenwaks S. // J. Appl. Phys. 1992. V. 72. P. 849.
15. Springer G. S., Wingeier E. W. / J. Chem. Phys. 1973. V. 59. P. 2747.

Laser Department Nuclear Research Center-Neger,
Israel

Поступила в редакцию
25 января 1993 г.